iScience

CellPress
OPEN ACCESS

Article

N-arachidonylglycine is a caloric state-dependent circulating metabolite which regulates human CD4^{+}T cell responsiveness

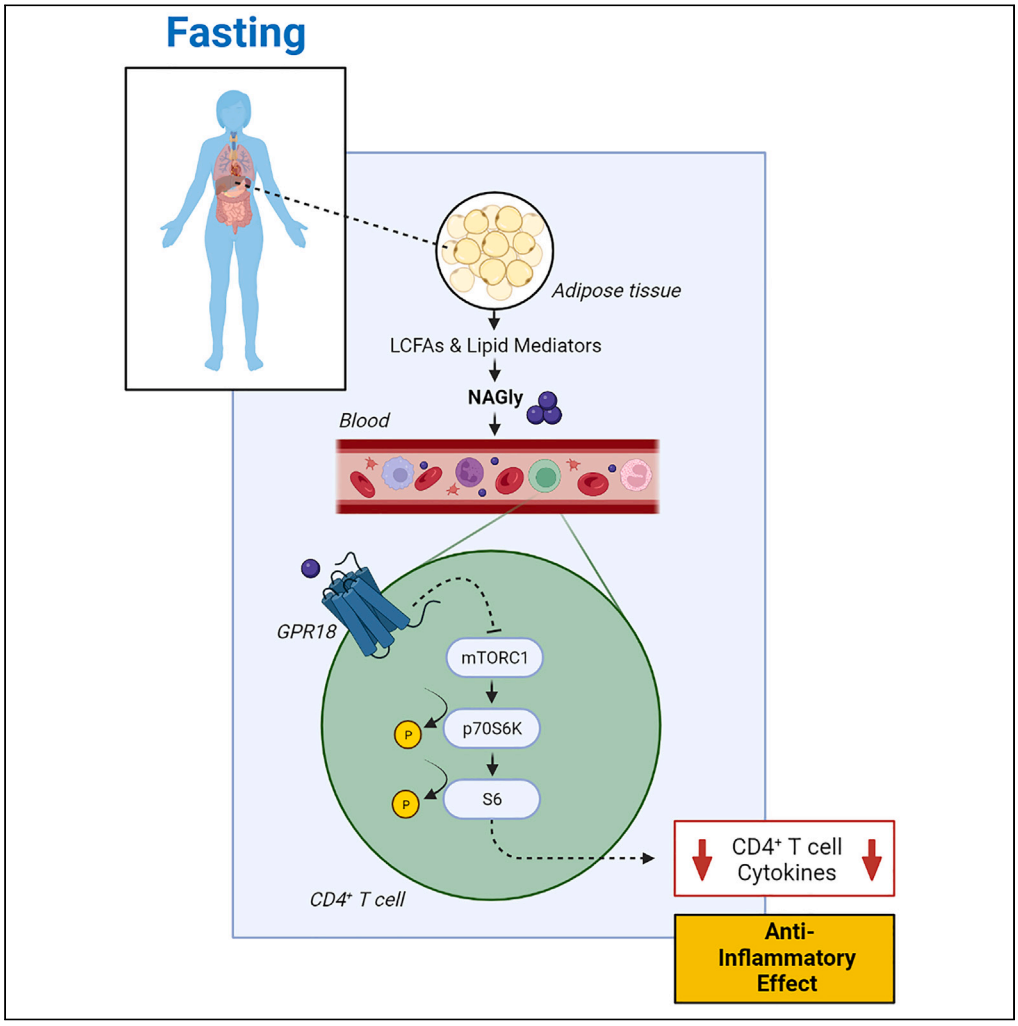

Allison M. Meadows, Kim Han, Komudi Singh, ..., Yvonne Baumer, Julian L. Griffin, Michael N. Sack

sackm@nih.gov

Highlights

A 24-h fast induces circulating levels of N-arachidonylglycine (NAGly)

NAGly has an anti-inflammatory effect in CD4^{+}T cells via GPR18 and MTORC1 signaling

NAGly effects are operational in T cells isolated from healthy and obese individuals

Meadows et al., iScience *26*, 106578
May 19, 2023
https://doi.org/10.1016/j.isci.2023.106578

iScience

CellPress
OPEN ACCESS

Article

N-arachidonylglycine is a caloric state-dependent circulating metabolite which regulates human CD4$^+$T cell responsiveness

Allison M. Meadows,[1,2] Kim Han,[1] Komudi Singh,[1] Antonio Murgia,[2] Ben D. McNally,[2] James A. West,[2] Rebecca D. Huffstutler,[3] Tiffany M. Powell-Wiley,[4] Yvonne Baumer,[4] Julian L. Griffin,[2,5] and Michael N. Sack[1,3,6,*]

SUMMARY

Caloric deprivation interventions such as intermittent fasting and caloric restriction ameliorate metabolic and inflammatory disease. As a human model of caloric deprivation, a 24-h fast blunts innate and adaptive immune cell responsiveness relative to the refed state. Isolated serum at these time points confers these same immunomodulatory effects on transformed cell lines. To identify serum mediators orchestrating this, metabolomic and lipidomic analysis was performed on serum extracted after a 24-h fast and re-feeding. Bioinformatic integration with concurrent peripheral blood mononuclear cells RNA-seq analysis implicated key metabolite-sensing GPCRs in fasting-mediated immunomodulation. The putative GPR18 ligand N-arachidonylglycine (NAGly) was elevated during fasting and attenuated CD4$^+$T cell responsiveness via GPR18 MTORC1 signaling. In parallel, NAGly reduced inflammatory Th1 and Th17 cytokines levels in CD4$^+$T cells isolated from obese subjects, identifying a fasting-responsive metabolic intermediate that may contribute to the regulation of nutrient-level dependent inflammation associated with metabolic disease.

INTRODUCTION

Nutrient excess has led to an epidemic of metabolic diseases, and caloric overconsumption gives rise to diverse systemic diseases, e.g., type II diabetes, non-alcoholic steatohepatitis, and increased cancer susceptibility.[1–3] Of interest, chronic inflammation is a common underlying pathophysiology linked to these caloric excess-initiated conditions. In contrast, caloric restriction and intermittent fasting interventions attenuate metabolic risk factors, reduce inflammation,[4,5] and enhance tumor surveillance.[6–11] Together, these data implicate immune regulation as an integral caloric-intake sensing system with profound effects on non-communicable degenerative disease development and/or prevention.

As intermittent fasting interventions are generally health-promoting, this acute dietary intervention is emerging as a useful human experimental model system to begin to explore the underlying regulatory mechanisms underpinning the anti-inflammatory effects of nutritional restriction. Diverse intracellular immune cell mechanisms have been identified, e.g., via chromatin remodeling,[12] gene transcription,[13] altered mitochondrial fidelity,[14] and through the regulation of canonical immune signal transduction pathways.[13] Paracrine or other extrinsic regulatory mechanisms following the release of regulatory proteins and metabolites into the circulation in response to fasting interventions are less well characterized. Caloric-load-dependent circulating metabolites, including the microbiome-generated short-chain fatty acid butyrate and β-hydroxybutyrate, generated by hepatic ketogenesis, both blunt the intracellular immune sensing NLRP3 inflammasome which is responsible for sterile inflammation,[15,16] and fasting-mediated secretion of IGFBP1 blunts T cell receptor (TCR) activated CD4$^+$T cell cytokines including IFNγ, IL-4 and IL-17.[17] Ultimately, integration of cell-autonomous and extrinsic regulatory pathways likely function in concert to alter the inflammatory milieu and contribute to the modulation of immune cell responsiveness to inflammatory triggers.

The objective of this study was to employ serum metabolomics and lipidomics to uncover circulating metabolites that may confer anti-inflammatory effects on CD4$^+$T cells in subjects that had been exposed to a fasting and re-feeding protocol, where our prior analyses focused on fasting-mediated blunting of

[1]Laboratory of Mitochondrial Biology and Metabolism, NHLBI, NIH, Bethesda, MD, USA

[2]Department of Biochemistry and Cambridge Systems Biology Centre, University of Cambridge, Cambridge, UK

[3]Cardiovascular Branch, NHLBI, NIH, Bethesda, MD, USA

[4]Social Determinants of Obesity and Cardiovascular Risk Laboratory, NHLBI, NIH, Bethesda, MD, USA

[5]The Rowett Institute, School of Medicine, Medical Sciences and Nutrition, Foresterhill Campus, Aberdeen, UK

[6]Lead contact

*Correspondence: sackm@nih.gov

https://doi.org/10.1016/j.isci.2023.106578

intracellular $CD4^+$ cell immune responsive gene regulation. Here, serum was secured from healthy volunteers exposed to a 24-h fast and 3 h of re-feeding as part of the initial clinical protocol where fasting was found to blunt $CD4^+$ T helper cell immune response via transcriptional regulatory mechanisms.[13] In this subsequent study, we aimed to identify fasting-induced circulating metabolites and characterize metabolite-signaling pathways in $CD4^+$T cells by integrating metabolomic and lipidomic analyses of collected serum in parallel with transcriptomic analyses from peripheral blood mononuclear cells (PBMCs) from the initial study at the same nutritional-load time points. Caloric load differentially regulated the levels of many serum metabolites and lipid species and the expression of multiple putative metabolite-sensing G-protein coupled receptors (GPCRs). By exploring identified ligands to metabolite-sensing GPCRs, we uncovered a fasting-associated anti-inflammatory signaling effect of the GPR18 ligand N-arachidonylglycine (NAGly) in $CD4^+$T cells isolated from normal volunteers. As a validation study, we demonstrated that this metabolite-derived anti-inflammatory effect was operational by comparing $CD4^+$T cells isolated from a separate cohort of lean versus obese subjects, indicating a potentially broader role for NAGly in immune modulation in different nutrient-load-associated metabolic diseases. By characterizing identified metabolites and metabolite-sensing pathways associated with prolonged fasting, we have uncovered a mechanism underpinning $CD4^+$T cell immune modulation, shed new light on the role of nutrient load on inflammatory pathophysiology, and uncovered a putative GPCR target to modulate $CD4^+$T cell immune responsiveness.

RESULTS

Serum metabolomics/lipidomics identify distinct circulatory metabolites comparing fasted to refed state

The demographics of the study subjects and the biochemical markers, including glucose, insulin, and growth hormone levels that support the distinct nutrient loads in the fasted versus the refed state are shown in Table S1. To identify potential paracrine signaling effects which confer anti-inflammatory effects of a 24-h fast, we employed a comprehensive metabolomic and lipidomic approach to explore changes to the serum metabolic profile after a 24-h fast compared to 3 h after re-feeding (Figure S1A). Serum LC-MS metabolomic analysis identified 66 polar metabolites and 170 distinct lipid species, and pairwise hypothesis testing identified significantly different levels of 26 polar metabolites and 44 lipids comparing fasting and re-feeding (Figure 1A, Table S2). Network analysis of the potential impact of these nutrient-dependent serum metabolite changes implicated differentially abundant metabolites in immunologic disease, inflammatory disease, and inflammatory response (Figure 1B). These results support the hypothesis that nutrient loads per se differentially modulate immune signaling and suggest an array of potential metabolite signaling intermediates which may confer immunoregulatory effects.

To begin to investigate which fasting-regulated metabolites confer nutrient-dependent immunomodulatory effects, we first employed orthogonal partial least squares-discriminant analysis (OPLS-DA) of metabolomic/lipidomic data. Serum samples, represented as the composite of all measured metabolites for each sample, were distinctly separated between fasted and refed groups ($R^2X = 0.31$, $R^2Y = 0.85$, $Q^2 = 0.76$, and cross-validation ANOVA $p = 5.50 \times 10^{-11}$), attributed to distinct fasting-mediated changes in the circulating plasma metabolome during fasting (Figure 1C). The OPLS-DA model was validated using a permutation plot (Figure S1B). Distinct metabolite biomarkers were identified using variable importance in prediction (VIP). Of the 70 differentially abundant metabolites, 51 had a VIP score greater than 1 (Table S2). The top VIP serum metabolites significantly increased by fasting were the long-chain fatty acids heptadecanoic acid (HDA, C17:0), arachidonic acid (AA, C20:4), oleic acid (OA, C18:1), and eicosapentaenoic acid (EPA, C20:5), as well as the polar metabolites uridine, acetyl-carnitine, and α-hydroxybutyrate (Figures 1D, S1C, and S1D). These metabolites have previously been identified as fasting biomarkers,[18–21] which validates our experimental model.

Bioinformatic integration of metabolite and transcript levels uncover putative ligand-receptor immunomodulatory signaling pathways

To identify putative immunomodulatory roles of fasting-induced metabolites, we then interrogated the RNA-seq database from PBMC samples from the same subjects (GSE165149).[13] Analysis at the 24-fast and 3-h re-feeding time points revealed a subset of 971 differentially expressed (DE, pvalue <0.05) genes (Figures S2A and S2B, Table S3). Gene Ontology (GO) enrichment analysis[22,23] supported that the biological process most significantly enriched pathway by fasting and re-feeding was the inflammatory response (Figure 2A). Of interest, the next two most enriched biological processes revealed differences in G-protein

A

Serum Metabolomics + Lipidomics		
	Detected metabolites (n)	Differentially expressed metabolites ($p < 0.05$) *Fasted vs. Refed*
Polar	66	26
Lipid	170	44
Total	236	70

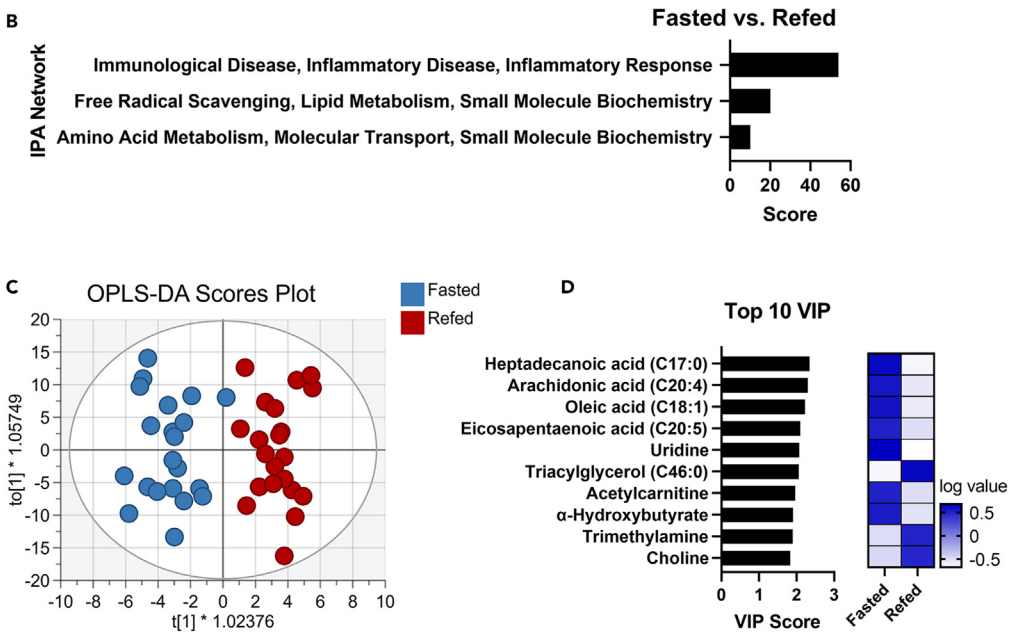

Figure 1. Metabolomics of human serum during fasting and re-feeding

(A) Number of serum metabolites detected by metabolomic and lipidomic analyses, and number of significantly different metabolites in fasted vs. refed pairwise comparisons. Hypothesis testing performed using a paired Wilcoxon signed-rank test (n = 21).

(B) Fasted versus refed network analysis of differentially abundant metabolites. Top three networks shown, ranked by enrichment score.

(C) OPLS-DA score scatterplot of serum samples from the fasted (blue) and refed (red) groups (n = 21 samples/group). $R^2X = 0.31$ $R^2Y = 0.85$. $Q^2 = 0.76$. P-value of the cross-validation ANOVA = 5.50×10^{-11}.

(D) Top 10 VIP metabolites and heatmap of mean log abundance in fasted and refed serum samples.

coupled receptor signaling (GPCR) and small GTPase-mediated signal transduction (Figure 2A). This was corroborated by GO molecular function analysis which showed enrichment in GPRC activity, GTP binding, and guanyl nucleotide binding (Figure 2B). Given that multiple metabolites signal through GPCRs,[24] these results suggested that GPCR signaling pathways may confer immune-modulatory effects of fasting and re-feeding. In this regard, 28 identified DE genes in the GPCR signaling pathway were identified (GO: 0007186) (Figure 2C). These included chemokine receptors, a known short-chain fatty acid receptor, and several receptors classified as orphan GPCRs. The orphan GPCR most highly regulated between fasting and re-feeding was GPR18 (Figures 2C and 2D), and emerging data support that GPR18 signaling may have immunomodulatory effects.[25–27]

Fasting-induced N-arachidonylglycine downregulates Th1 and Th17 immune responsiveness

Of interest, the N-acyl amino acid (nAAA) N-arachidonylglycine (NAGly) has been identified as a potential GPR18 ligand,[28] and its lipid precursor arachidonic acid was identified as the top metabolite distinguishing the fasted from the refed state (Figure 1D). We therefore directly measured the levels of NAGly, which is a conjugate of arachidonic acid with glycine,[29] by LC-MS/MS. NAGly levels were markedly increased during fasting compared to matched refed serum levels (Figure 3A). Significant correlation between the serum abundance of NAGly and arachidonic acid ($R^2 = 0.53$, $p = 0.017$) suggested that NAGly may be derived

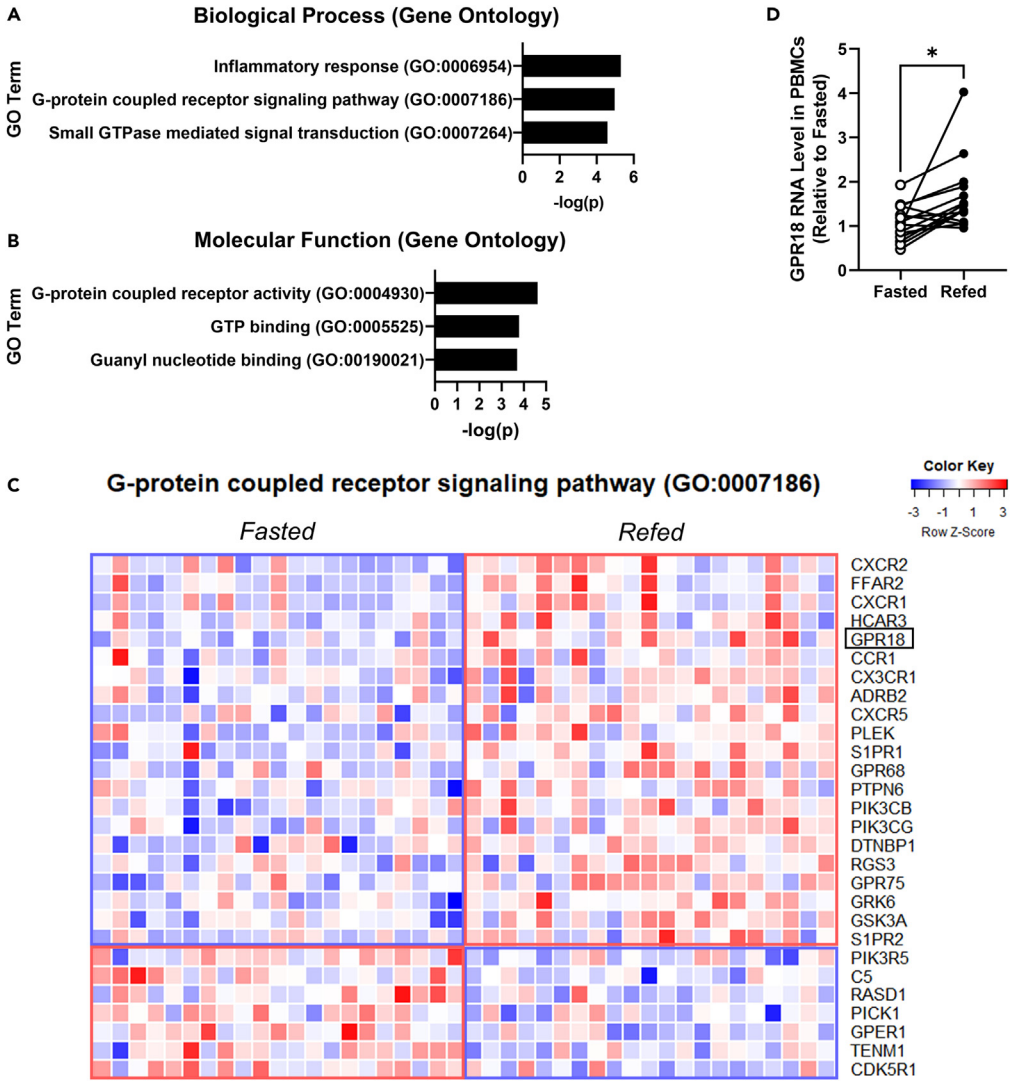

Figure 2. PBMC RNA-seq of PBMCs in the fasted and refed state

(A and B) Biological process and (B) molecular function GO analysis of 971 DE genes from PBMCs. Top 3 enriched processes shown, ranked by the inverse log of the p-value.

(C) Relative expression of 28 DE genes ($p < 0.05$) enriched in the G-protein coupled receptor signaling pathway (GO: 0007186). Gene expression (FPKM, Fragments Per Kilobase of transcript per Million) indicated by row Z-score as relative increase (red) or decrease (blue). Samples (x-axis) grouped by fasted and refed timepoints. Genes (y-axis) ranked by mean fold change.

(D) GPR18 RNA expression in PBMCs collected at fasting and re-feeding timepoints (relative to the mean of fasted group, n = 15/group). Significance using a paired t-test, * - $p < 0.05$.

from or regulated in parallel with arachidonic acid during fasting (Figure 3B). To evaluate whether NAGly could function as an extracellular signaling molecule, we assayed its stability in $CD4^+$T cell culture media over three days. NAGly levels remained relatively constant (Figures S3A and S3B), which could implicate its role as a potential immunomodulatory signaling molecule.

As the 24-h fast has a robust effect on blunting $CD4^+$ effector T cell signaling, in parallel with the induction of NAGly and associated cytokine production, and given that GPR18 expression in primary $CD4^+$T cells is differentially regulated by fasting and re-feeding (Figure 3C), we sought to assess the potential immunomodulatory effects of the putative NAGly-GPR18 nexus on $CD4^+$T cells. NAGly was studied at a concentration of 10 μM,[30,31] which did not reduce the viability of primary $CD4^+$T cells (Figure S3C). In parallel, NAGly

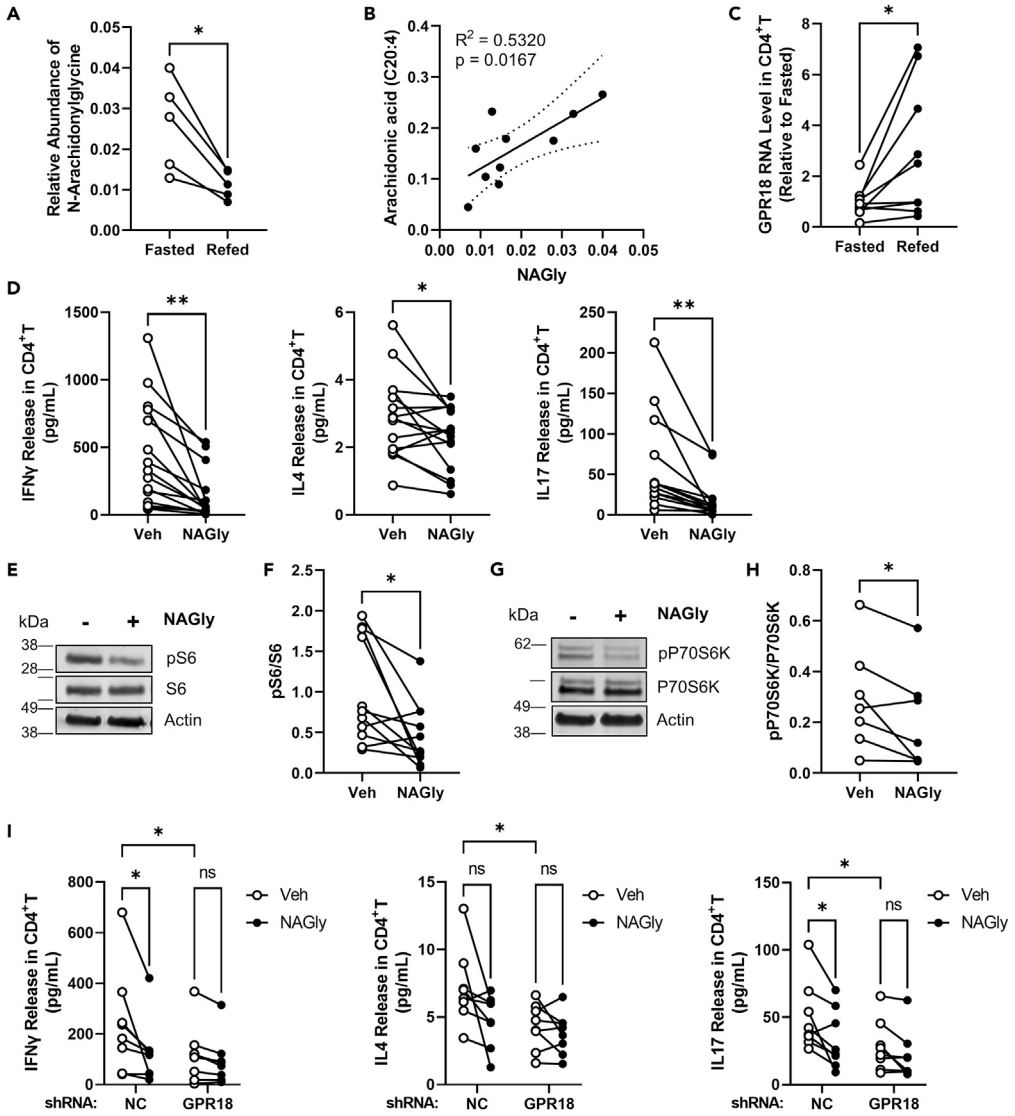

Figure 3. Functional characterization of NAGly/GPR18 signaling in CD4$^+$T cells

(A) Relative abundance of NAGly in human serum collected at fasted and refed timepoints (n = 5).

(B) Pearson correlation of NAGly and arachidonic acid relative abundance in matched serum samples (n = 10). Line of best fit and 95% confidence intervals shown.

(C) RNA expression of GPR18 in CD4$^+$T cells isolated from PBMC samples collected at fasted and refed timepoints (relative to the mean of fasted group, n = 9/group).

(D) Release of IFNγ, IL-4, and IL-17 cytokines from CD4$^+$T cells treated with 10 μM NAGly relative to vehicle control (n = 15).

(E) S6 protein and phosphoprotein abundance in CD4$^+$T cells treated with 10 μM NAGly relative to vehicle control.

(F) Quantification of immunoblot: pS6/S6 (n = 11).

(G) P70S6K protein and phosphoprotein abundance in CD4$^+$T cells treated with 10 μM NAGly relative to vehicle control.

(H) pP70S6K/P70S6K (n = 7).

(I) Release of IFNγ, IL-4, and IL-17 cytokines from CD4$^+$T cells treated with GPR18 shRNA or negative control +/− 10 μM NAGly (n = 8). Significance using a paired Student's *t* test, or by a two-way ANOVA with Tukey's multiple comparisons test. * - $p < 0.05$, ** - $p < 0.01$.

decreased transcript levels of genes encoding canonical T cell transcription factors (TF) TBX21 (T-bet, Th1 specific TF) and RORC (RORγt, Th17 specific TF), but not GATA3 (Th2 specific TF) (Figure S3D). Furthermore, NAGly administration significantly blunted IFNγ and IL-17 secretion with a less robust effect on

IL-4 secretion (Figure 3D). Together, these data support a regulatory role of NAGly in blunting Th1/Th17 rather than Th2 inflammatory signaling.

Fasting-associated CD4$^+$T cell inflammatory signaling is partly mediated by mTOR and the STAT family of transcription and translation regulatory proteins, STAT1 and STAT3.[13] Of interest, neither STAT1 nor STAT3 phosphoprotein levels were significantly affected by NAGly, implicating that the potential anti-inflammatory mechanism was independent of the JAK-STAT signaling cascade (FiguresS3E–S3H). In contrast, the administration of NAGly decreased phosphorylation of MTORC1 effectors P70S6K and ribosomal protein S6 (Figures 3E–3H), supporting that NAGly could blunt signaling downstream of MTORC1, ultimately conferring reduced Th1 and Th17 immune responsiveness. To assess whether this NAGly effect was via GPR18, the receptor agonist PSB-KD107 (KD107)[32] was studied. KD107 incubation similarly blunted IFNγ and IL-17, but not IL-4 secretion (Figures S4A and S4B). In addition, KD107 significantly blunted phosphorylation of ribosomal protein S6 but not P70S6K (Figures S4C–S4F), suggesting that GPR18 agonism partially reproduces the anti-inflammatory effect of NAGly by blunting MTORC1 signaling. Conversely, antagonism of GPR18 with PSB-CB5[33,34] did not modulate the release of IFNγ and IL-17 cytokines, although it did induce IL-4 secretion (Figures S4G and S4H). These findings support that GPR18 activation may replicate the anti-inflammatory effect of NAGly in Th1 and Th17 cells and that GPR18 inhibition may have the opposite effect with respect to Th2-linked cytokine release. To explore this further, lentiviral-transduced short hairpin RNA (shRNA) targeting GPR18 was investigated. In primary CD4$^+$T cells, a ≈50% knockdown of GPR18 transcript levels was achieved vs. scrambled control knockdown (Figure S4I). As may be expected, NAGly significantly decreased IFNγ and IL-17, but not IL-4, in scrambled control cells, whereas GPR18 knockdown blunted these effects. Of interest, knockdown of GPR18 alone diminished IFNγ, IL-4, and IL-17 release (Figure 3I).

NAGly levels correlate with chronic nutrient load states with parallel immunomodulatory effects

As immune-modulatory changes associated with fasting and re-feeding may be relevant to the inflammatory pathophysiology of metabolic disease, especially obesity,[17] we then analyzed RNA-seq data of subcutaneous adipose tissue biopsies collected from human volunteers classified as lean or obese (GEO ID: GSE166047)[35] to investigate whether there was a parallel GPRC pathway regulation. Analysis revealed a large subset of DE genes comparing lean and obese samples (Figure 4A). In line with our findings, GO analysis uncovered enrichment of DE genes linked to leukocyte and lymphocyte activation and inflammatory response (Figure 4B) as well as enrichment in G-protein coupled receptor activity (Figure 4C). Based on this, we then evaluated whether NAGly affected CD4$^+$T cell responsiveness in lean and obese volunteers we had previously studied.[17] The subjects' demographics and differences in body mass index (BMI) are shown in Table S4. In CD4$^+$T cells, GPR18 expression was upregulated in the obese cohort (Figure 4D), which is interesting considering it is also upregulated by re-feeding. NAGly supplementation also significantly blunted IFNγ release in CD4$^+$T cells isolated from obese individuals and IL-17 release in both lean and obese samples, whereas it did not affect IL-4 release in either group (Figure 4E). At the same time, the comparison of NAGly/GPR18 biology between an acute intervention (fasting/re-feeding) with a more steady-state body weight (lean versus obese) is complex and does not account for a myriad of variables that exist between the different cohorts. To uncover this, albeit, at a reductionist level, we subdivided the fasting/re-feeding cohort into normal and increased BMI and compared GPR18 transcript levels and circulating levels of arachidonic acid. Of interest, the differential expression of GPR18 and arachidonic level between fasting and re-feeding were retained irrespective of the subjects' BMI (Figures S5A and S5B). Together, these findings further support that NAGly has the potential to blunt CD4$^+$T cell activation in different metabolic states, further reinforcing its regulatory role in an inflammatory milieu.

DISCUSSION

This study employed a 24-h fasting and 3-h re-feeding protocol in healthy volunteers to identify circulating nutrient-level dependent metabolites that function as immune mediators. Integrating these data with PBMC RNA-seq analysis from the same subjects and subsequent biologic pathway interrogation uncovered that the caloric load-responsive metabolite NAGly, signaling via the orphan G-protein coupled receptor GPR18, blunted Th1 and Th17 immune responsiveness in primary CD4$^+$T cells from healthy subjects, a finding then validated in obese subjects. These data add to our understanding of how a circulating conjugated lipid-amino acid species contributes through GPCR signaling to remodel CD4$^+$T cell immune responsiveness.

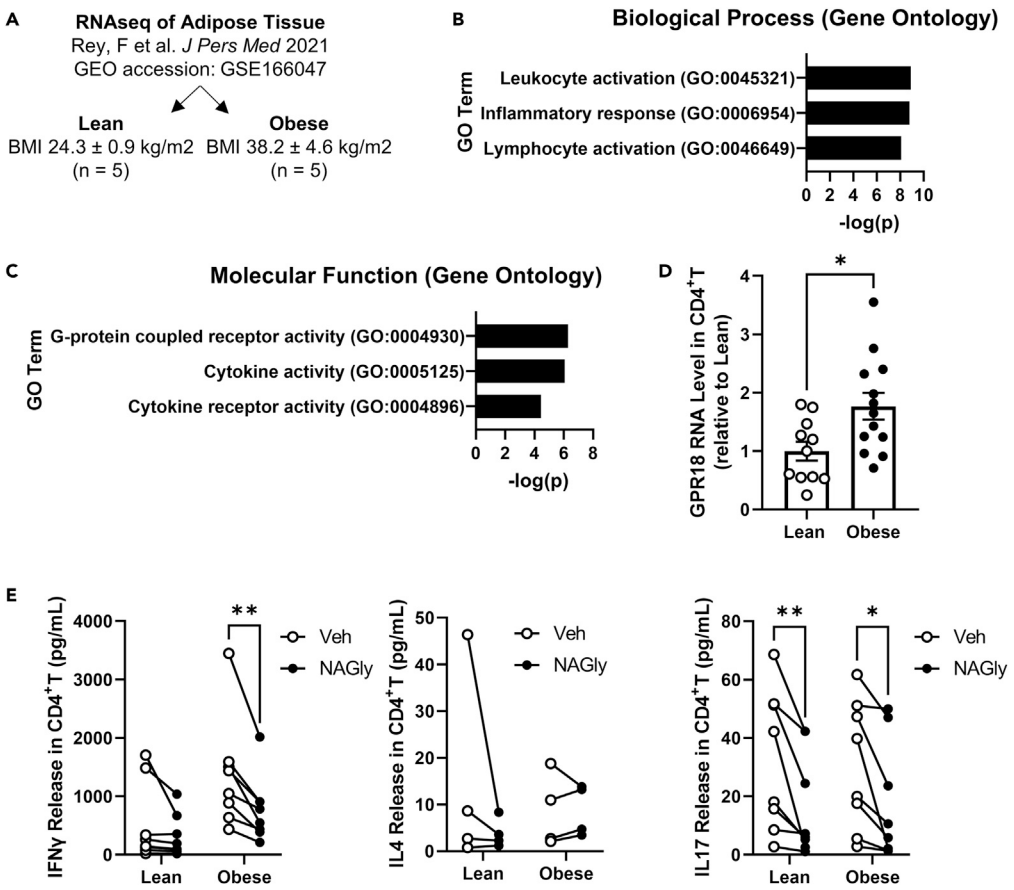

Figure 4. NAGly anti-inflammatory effects are GPR18-dependent and operational in obesity

(A) RNA sequencing of subcutaneous adipose tissue biopsy collected from 10 female volunteers without T2DM classified as lean (n = 5) or obese (n = 5).

(B and C) Biological process and (C) molecular function GO analysis of DE genes. Top 3 enriched processes shown, ranked by the inverse log of the p value.

(D) Relative expression of GPR18 in naive primary CD4$^+$ T cells isolated from PBMCs collected from lean (n = 10) or obese (n = 10) volunteers. RNA expression normalized to 18S ribosomal RNA (relative expression to the mean of the lean group). Significance using an unpaired t-test.

(E) Release of IFNγ, IL-4, and IL-17 cytokines from αCD3/αCD28 antibody-activated CD4$^+$T cells treated with 10 μM NAGly relative to vehicle control (n = 4–8). Cytokines measured by ELISA immunoassay and normalized to cell density by CyQuant assay. Significance reported using a two-way ANOVA with Šídák's multiple comparisons test. [*] indicates $p < 0.05$. [**] indicates $p < 0.01$.

Although the circulating levels of numerous hydrophilic and lipid metabolites differed in the fasted and refed state, this study focused on NAGly given that its levels were induced by fasting and in that its immunomodulatory role is not well established. In addition, its putative receptor GPR18 is expressed throughout the body, with elevated levels in the spleen and other lymph tissue, indicating a potential role in regulating immune activity.[36] At the same time, genome-wide association studies identify GPR18 as a biomarker of disease with immunologic involvement, including sepsis and asthma.[37–40] Prior data had shown that NAGly reduced PBMC IL-1β cytokine secretion.[31] In addition, the NAGly/GPR18 nexus had been explored in the context of innate immune cell survival and migration.[30,41,42] In adaptive immunity, GPR18 was found to maintain intestinal CD8$^+$ intraepithelial lymphocyte integrity[25,26] and modulate CD8$^+$ effector-memory T cell compartmentalization,[27] although in those studies NAGly was not explored. NAGly has also been identified as a ligand for GPR18,[28] and GPR18 is necessary for NAGly signaling effects.[30,41–46] The pharmacologic and GPR18 knockdown data in this study extends this knowledge showing that NAGly has distinct Th1 and Th17 anti-inflammatory effects as a ligand for the GPR18 receptor. At the same time, GPR18 has been found to be constitutively active.[40,47] Of interest, a concept supported in our study suggests that

the constitutive effect of GPR18 is pro-inflammatory in $CD4^+$T cells, given that its knockdown blunted IFNγ, IL-4, and IL-17 levels in the absence of NAGly supplementation. The finding that the transcript encoding GPR18 was induced by re-feeding in $CD4^+$T cells could be consistent with this regulation, although further studies are required to explore this putative feedforward regulation. The pharmacologic data is less consistent, though, given that the GPR18 agonist PSB-KD107 blunted IFNγ and IL-17 release, whereas the antagonist augmented IL-4 secretion. This latter finding does not align with either the global effect of GPR18 KD or in opposition to the effect of NAGly administration.

At a signaling level, NAGly supplementation has been shown to increase levels of anti-inflammatory eicosanoids, including lipoxin A_4 and prostaglandin J^2 in GPR18-transfected HEK393 cells,[45] suggesting that this signaling cascade may function through these lipid mediators. In this study, we explored the effects of NAGly on canonical T cell signaling by evaluating MTORC1 and STAT signaling. We found that NAGly blunted the phosphorylation of p70S6K and ribosomal pS6. These replicated the fasting effect on Th1 and Th17 regulation and the role of the MTORC1 pathway,[13] and is consistent with data showing that the nutrient-sensing MTORC1 pathway promotes Th1/Th17 cell subsets activation while inhibiting Th2 cells and Tregs.[48] The GPR18 agonist did not faithfully replicate this data with a more robust effect on blunting pS6 but not p70S6K. Why the ribosomal MTORC1 pathway was more responsive to this agonist remains unclear. In contrast, NAGly did not blunt signaling through the STAT1 and STAT3 pathways, which are also mechanistically linked to Th1 and Th17 immune responsiveness. However, genetic knockout studies have shown that STAT1 and STAT3 independent mechanisms regulate Th1 and Th17 cytokines.[49–51]An important caveat here is that these STAT1/3 independent mechanisms do not fully enable complete immune fidelity of these cell types suggesting that the functional *in vivo* effect of NAGly and GPR18 would need to be assessed more broadly in the context of $CD4^+$ T helper cell immune functioning.

At the same time, the fact that NAGly reduced the production of IFNγ and IL-17 in $CD4^+$T cells isolated from lean and obese volunteers further supports that NAGly confers anti-inflammatory effects. These data point to an interesting putative GPCR-linked pathway that may be targeted in managing chronic inflammation of metabolic syndrome-linked diseases and highlight that the role of the circulating metabolome in modulating metabolic-linked diseases needs to be understood in more detail to uncover potential mechanisms whereby nutritional intervention may improve health in these diseases. At the same time, the finding that GPR18 levels were differentially expressed in the lean versus obese cohorts, implicates that this signaling may be operational in more chronic nutrient-level dependent states linked to sterile inflammation. However, the complexity of this regulation and potential dynamics linked to weight are completely unexplored and would need to be addressed.

In conclusion, we have identified the NAGly-GPR18 nexus as a metabolite and metabolite-sensing pathway in $CD4^+$T cell immunoregulation in response to fasting. Future studies should further uncover how endogenous signaling metabolites control inflammatory signaling to advance our understanding of mechanisms underpinning fasting-mediated immune modulation. This study reinforces the concept that circulating metabolites effects of dietary manipulation, from either the gut microbiome response or by release from solid organs such as the liver, skeletal muscle, and adipocytes, have immunomodulatory effects. Our advancing appreciation of the signaling role of these metabolites will ultimately contribute to an improved understanding of the integration of metabolism and immune health, informing a targeted nutritional and therapeutic approach to treating metabolic and inflammatory diseases.

Limitations of the study

The limitations of this study were that we explored only one of many circulating metabolites altered by fasting in modulating immune responsiveness and focused on one lymphocytic cell lineage. In addition, our initial metabolomics screen examined only a limited number of metabolites, and other metabolites with regulatory roles need to be defined. This study also uncovered the potential paradox of elevated NAGly levels in the fasted state but elevated GPCR18 expression in the refed state, which will need to be explored in greater depth to understand their interplay and regulatory effects. Further studies into NAGly-GPR18 signaling will need to be explored across different innate and adaptive immune cells known to be nutrient-responsive. Furthermore, serum samples should be acquired from population studies exploring nutrient-responsive diseases to evaluate if targeting this pathway could have immune-responsive effects.

STAR★METHODS

Detailed methods are provided in the online version of this paper and include the following:

- KEY RESOURCES TABLE
- RESOURCE AVAILABILITY
  - Lead contact
  - Materials availability
  - Data and code availability
- EXPERIMENTAL MODEL AND SUBJECT DETAILS
  - Fasting/re-feeding study
  - Lean/obese study
  - Healthy volunteers
- METHOD DETAILS
  - LC-MS of serum samples
  - Computational analysis of metabolomics data
  - Computational analysis of transcriptomics data
  - Functional validation in primary $CD4^+$T cells
- QUANTIFICATION AND STATISTICAL ANALYSIS
- ADDITIONAL RESOURCES

SUPPLEMENTAL INFORMATION

Supplemental information can be found online at https://doi.org/10.1016/j.isci.2023.106578.

ACKNOWLEDGMENTS

We thank Drs. Zoe Hall and Sonia Liggi of the University of Cambridge Biochemistry Department for their contributions to metabolomics analysis and data processing. Shahin Hassanzadeh of the Laboratory of Mitochondrial Biology and Metabolism for developing the PBMC RNAseq library.Matthew Rodman of the Laboratory of Mitochondrial Biology and Metabolism for preparing lean/obese samples. Dr. Duck-Yeon Lee of the NHLBI Biochemistry Core for NAGly analysis in cell culture. Special thanks to the National Institutes of Health Oxford-Cambridge Scholars Program and the International Biomedical Research Alliance for their sponsorship and support.

Funding: NHLBI Division of Intramural Research (MNS – ZIA-HL005199) and the UK MRC (JLG – MR/P011705/2; UKDRI-5002; MAPUK).

AUTHOR CONTRIBUTIONS

Conceptualization, A.M.M., J.L.G., and M.N.S.; Methodology, A.M.M., K.H., K.S., A.M., J.L.G., and M.N.S.; Formal Analysis, A.M.M., K.H., and K.S.; Investigation, A.M.M., K.H., A.M., B.D.M., and J.A.W.; Resources, R.H., T.M.P-W., and Y.B.; Writing – Original Draft, A.M.M. and M.N.S.; Writing – Review & Editing, K.H., K.S., and J.L.G.; Supervision, J.L.G. and M.N.S.; Funding Acquisition, J.L.G. and M.N.S.

DECLARATION OF INTERESTS

The authors declare no competing interests.

INCLUSION AND DIVERSITY

We support inclusive, diverse, and equitable conduct of research.

Received: October 17, 2022
Revised: January 29, 2023
Accepted: March 29, 2023
Published: April 6, 2023

REFERENCES

1. Saklayen, M.G. (2018). The global epidemic of the metabolic syndrome. Curr.Hypertens.Rep. *20*, 12. https://doi.org/10.1007/s11906-018-0812-z.

2. Lee, Y.S., and Olefsky, J. (2021). Chronic tissue inflammation and metabolic disease. Genes Dev. *35*, 307–328. https://doi.org/10.1101/gad.346312.120.

3. Avgerinos, K.I., Spyrou, N., Mantzoros, C.S., and Dalamaga, M. (2019). Obesity and cancer risk: emerging biological mechanisms and perspectives. Metabolism *92*, 121–135. https://doi.org/10.1016/j.metabol.2018.11.001.

4. Stekovic, S., Hofer, S.J., Tripolt, N., Aon, M.A., Royer, P., Pein, L., Stadler, J.T., Pendl, T., Prietl, B., Url, J., et al. (2019). Alternate day fasting improves physiological and molecular markers of aging in healthy, non-obese humans. Cell Metabol. *30*, 462–476.e6. https://doi.org/10.1016/j.cmet.2019.07.016.

5. Wang, X., Yang, Q., Liao, Q., Li, M., Zhang, P., Santos, H.O., Kord-Varkaneh, H., and Abshirini, M. (2020). Effects of intermittent fasting diets on plasma concentrations of inflammatory biomarkers: a systematic review and meta-analysis of randomized controlled trials. Nutrition *79–80*, 110974. https://doi.org/10.1016/j.nut.2020.110974.

6. Wei, M., Brandhorst, S., Shelehchi, M., Mirzaei, H., Cheng, C.W., Budniak, J., Groshen, S., Mack, W.J., Guen, E., Di Biase, S., et al. (2017). Fasting-mimicking diet and markers/risk factors for aging, diabetes, cancer, and cardiovascular disease. Sci. Transl. Med. *9*, eaai8700. https://doi.org/10.1126/scitranslmed.aai8700.

7. Patterson, R.E., and Sears, D.D. (2017). Metabolic effects of intermittent fasting. Annu. Rev. Nutr. *37*, 371–393. https://doi.org/10.1146/annurev-nutr-071816-064634.

8. Mattson, M.P., Longo, V.D., and Harvie, M. (2017). Impact of intermittent fasting on health and disease processes. Ageing Res. Rev. *39*, 46–58. https://doi.org/10.1016/j.arr.2016.10.005.

9. Park, J., Seo, Y.G., Paek, Y.J., Song, H.J., Park, K.H., and Noh, H.M. (2020). Effect of alternate-day fasting on obesity and cardiometabolic risk: a systematic review and meta-analysis. Metabolism *111*, 154336. https://doi.org/10.1016/j.metabol.2020.154336.

10. Tinsley, G.M., and La Bounty, P.M. (2015). Effects of intermittent fasting on body composition and clinical health markers in humans. Nutr. Rev. *73*, 661–674. https://doi.org/10.1093/nutrit/nuv041.

11. Fontana, L., Meyer, T.E., Klein, S., and Holloszy, J.O. (2004). Long-term calorie restriction is highly effective in reducing the risk for atherosclerosis in humans. Proc. Natl. Acad. Sci. USA *101*, 6659–6663. https://doi.org/10.1073/pnas.0308291101.

12. Goldstein, I., and Hager, G.L. (2015). Transcriptional and chromatin regulation during fasting - the genomic era. Trends Endocrinol.Metabol. *26*, 699–710. https://doi.org/10.1016/j.tem.2015.09.005.

13. Han, K., Singh, K., Rodman, M.J., Hassanzadeh, S., Wu, K., Nguyen, A., Huffstutler, R.D., Seifuddin, F., Dagur, P.K., Saxena, A., et al. (2021). Fasting-induced FOXO4 blunts human CD4(+) T helper cell responsiveness. Nat. Metab. *3*, 318–326. https://doi.org/10.1038/s42255-021-00356-0.

14. Traba, J., Kwarteng-Siaw, M., Okoli, T.C., Li, J., Huffstutler, R.D., Bray, A., Waclawiw, M.A., Han, K., Pelletier, M., Sauve, A.A., et al. (2015). Fasting and refeeding differentially regulate NLRP3 inflammasome activation in human subjects. J. Clin. Invest. *125*, 4592–4600. https://doi.org/10.1172/JCI83260.

15. Youm, Y.H., Nguyen, K.Y., Grant, R.W., Goldberg, E.L., Bodogai, M., Kim, D., D'Agostino, D., Planavsky, N., Lupfer, C., Kanneganti, T.D., et al. (2015). The ketone metabolite beta-hydroxybutyrate blocks NLRP3 inflammasome-mediated inflammatory disease. Nat. Med. *21*, 263–269. https://doi.org/10.1038/nm.3804.

16. Wang, X., He, G., Peng, Y., Zhong, W., Wang, Y., and Zhang, B. (2015). Sodium butyrate alleviates adipocyte inflammation by inhibiting NLRP3 pathway. Sci. Rep. *5*, 12676. https://doi.org/10.1038/srep12676.

17. Han, K., Singh, K., Rodman, M.J., Hassanzadeh, S., Baumer, Y., Huffstutler, R.D., Chen, J., Candia, J., Cheung, F., Stagliano, K.E.R., et al. (2021). Identification and validation of nutrient state-dependent serum protein mediators of human CD4(+) T cell responsiveness. Nutrients *13*, 1492. https://doi.org/10.3390/nu13051492.

18. Steinhauser, M.L., Olenchock, B.A., O'Keefe, J., Lun, M., Pierce, K.A., Lee, H., Pantano, L., Klibanski, A., Shulman, G.I., Clish, C.B., and Fazeli, P.K. (2018). The circulating metabolome of human starvation. JCI Insight *3*, e121434. https://doi.org/10.1172/jci.insight.121434.

19. Deng, Y., Wang, Z.V., Gordillo, R., An, Y., Zhang, C., Liang, Q., Yoshino, J., Cautivo, K.M., De Brabander, J., Elmquist, J.K., et al. (2017). An adipo-biliary-uridine axis that regulates energy homeostasis. Science *355*, eaaf5375. https://doi.org/10.1126/science.aaf5375.

20. Costa, C.C., de Almeida, I.T., Jakobs, C., Poll-The, B.T., and Duran, M. (1999). Dynamic changes of plasma acylcarnitine levels induced by fasting and sunflower oil challenge test in children. Pediatr. Res. *46*, 440–444. https://doi.org/10.1203/00006450-199910000-00013.

21. Rubio-Aliaga, I., de Roos, B., Duthie, S.J., Crosley, L.K., Mayer, C., Horgan, G., Colquhoun, I.J., Le Gall, G., Huber, F., Kremer, W., et al. (2010). Metabolomics of prolonged fasting in humans reveals new catabolic markers. Metabolomics *7*, 375–387. https://doi.org/10.1007/s11306-010-0255-2.

22. Gene Ontology Consortium (2021). The Gene Ontology resource: enriching a GOld mine. Nucleic Acids Res. *49*, D325–D334. https://doi.org/10.1093/nar/gkaa1113.

23. Ashburner, M., Ball, C.A., Blake, J.A., Botstein, D., Butler, H., Cherry, J.M., Davis, A.P., Dolinski, K., Dwight, S.S., Eppig, J.T., et al. (2000). Gene ontology: tool for the unification of biology. The Gene Ontology Consortium. Nat. Genet. *25*, 25–29. https://doi.org/10.1038/75556.

24. Husted, A.S., Trauelsen, M., Rudenko, O., Hjorth, S.A., and Schwartz, T.W. (2017). GPCR-mediated signaling of metabolites. Cell Metabol. *25*, 777–796. https://doi.org/10.1016/j.cmet.2017.03.008.

25. Becker, A.M., Callahan, D.J., Richner, J.M., Choi, J., DiPersio, J.F., Diamond, M.S., and Bhattacharya, D. (2015). GPR18 controls reconstitution of mouse small intestine intraepithelial lymphocytes following bone marrow transplantation. PLoS One *10*, e0133854. https://doi.org/10.1371/journal.pone.0133854.

26. Wang, X., Sumida, H., and Cyster, J.G. (2014). GPR18 is required for a normal CD8αα intestinal intraepithelial lymphocyte compartment. J. Exp. Med. *211*, 2351–2359. https://doi.org/10.1084/jem.20140646.

27. Sumida, H., and Cyster, J.G. (2018). G-protein coupled receptor 18 contributes to establishment of the CD8 effector T cell compartment. Front. Immunol. *9*, 660. https://doi.org/10.3389/fimmu.2018.00660.

28. Kohno, M., Hasegawa, H., Inoue, A., Muraoka, M., Miyazaki, T., Oka, K., and Yasukawa, M. (2006). Identification of N-arachidonylglycine as the endogenous ligand for orphan G-protein-coupled receptor GPR18. Biochem.Biophys. Res. Commun. *347*, 827–832. https://doi.org/10.1016/j.bbrc.2006.06.175.

29. Bradshaw, H.B., Rimmerman, N., Hu, S.S.J., Benton, V.M., Stuart, J.M., Masuda, K., Cravatt, B.F., O'Dell, D.K., and Walker, J.M. (2009). The endocannabinoid anandamide is a precursor for the signaling lipid N-arachidonoyl glycine by two distinct pathways. BMC Biochem. *10*, 14. https://doi.org/10.1186/1471-2091-10-14.

30. McHugh, D., Hu, S.S.J., Rimmerman, N., Juknat, A., Vogel, Z., Walker, J.M., and Bradshaw, H.B. (2010). N-arachidonoyl glycine, an abundant endogenous lipid, potently drives directed cellular migration through GPR18, the putative abnormal cannabidiol receptor. BMC Neurosci. *11*, 44. https://doi.org/10.1186/1471-2202-11-44.

31. Burstein, S.H., Rossetti, R.G., Yagen, B., and Zurier, R.B. (2000). Oxidative metabolism of anandamide. Prostag.Other Lipid Mediat. *61*, 29–41. https://doi.org/10.1016/s0090-6980(00)00053-8.

32. Schoeder, C.T., Mahardhika, A.B., Drabczyńska, A., Kieć-Kononowicz, K., and Müller, C.E. (2020). Discovery of tricyclic

xanthines as agonists of the cannabinoid-activated orphan G-protein-coupled receptor GPR18. ACS Med. Chem. Lett. *11*, 2024–2031. https://doi.org/10.1021/acsmedchemlett.0c00208.

33. Rempel, V., Atzler, K., Behrenswerth, A., Karcz, T., Schoeder, C., Hinz, S., Kaleta, M., Thimm, D., Kiec-Kononowicz, K., and Müller, C.E. (2014). Bicyclic imidazole-4-one derivatives: a new class of antagonists for the orphan G protein-coupled receptors GPR18 and GPR55. MedChemComm *5*, 632–649. https://doi.org/10.1039/C3MD00394A.

34. Flegel, C., Vogel, F., Hofreuter, A., Wojcik, S., Schoeder, C., Kieć-Kononowicz, K., Brockmeyer, N.H., Müller, C.E., Becker, C., Altmüller, J., et al. (2016). Characterization of non-olfactory GPCRs in human sperm with a focus on GPR18. Sci. Rep. *6*, 32255. https://doi.org/10.1038/srep32255.

35. Rey, F., Messa, L., Pandini, C., Maghraby, E., Barzaghini, B., Garofalo, M., Micheletto, G., Raimondi, M.T., Bertoli, S., Cereda, C., et al. (2021). RNA-Seq characterization of sex-differences in adipose tissue of obesity affected patients: computational analysis of differentially expressed coding and non-coding RNAs. J. Personalized Med. *11*, 352. https://doi.org/10.3390/jpm11050352.

36. Gantz, I., Muraoka, A., Yang, Y.K., Samuelson, L.C., Zimmerman, E.M., Cook, H., and Yamada, T. (1997). Cloning and chromosomal localization of a gene (GPR18) encoding a novel seven transmembrane receptor highly expressed in spleen and testis. Genomics *42*, 462–466. https://doi.org/10.1006/geno.1997.4752.

37. Zhang, L., Qiu, C., Yang, L., Zhang, Z., Zhang, Q., Wang, B., and Wang, X. (2019). GPR18 expression on PMNs as biomarker for outcome in patient with sepsis. Life Sci. *217*, 49–56. https://doi.org/10.1016/j.lfs.2018.11.061.

38. Ferguson, B., Bokka, N.R., Maddipati, K.R., Ayilavarapu, S., Weltman, R., Zhu, L., Chen, W., Zheng, W.J., Angelov, N., Van Dyke, T.E., and Lee, C.T. (2020). Distinct profiles of specialized pro-resolving lipid mediators and corresponding receptor gene expression in periodontal inflammation. Front. Immunol. *11*, 1307. https://doi.org/10.3389/fimmu.2020.01307.

39. Valette, K., Li, Z., Bon-Baret, V., Chignon, A., Bérubé, J.C., Eslami, A., Lamothe, J., Gaudreault, N., Joubert, P., Obeidat, M., et al. (2021). Prioritization of candidate causal genes for asthma in susceptibility loci derived from UK Biobank. Commun.Biol. *4*, 700. https://doi.org/10.1038/s42003-021-02227-6.

40. Qin, Y., Verdegaal, E.M.E., Siderius, M., Bebelman, J.P., Smit, M.J., Leurs, R., Willemze, R., Tensen, C.P., and Osanto, S. (2011). Quantitative expression profiling of G-protein-coupled receptors (GPCRs) in metastatic melanoma: the constitutively active orphan GPCR GPR18 as novel drug target. Pigment Cell Melanoma Res. *24*, 207–218. https://doi.org/10.1111/j.1755-148X.2010.00781.x.

41. Takenouchi, R., Inoue, K., Kambe, Y., and Miyata, A. (2012). N-arachidonoyl glycine induces macrophage apoptosis via GPR18. Biochem.Biophys. Res. Commun. *418*, 366–371. https://doi.org/10.1016/j.bbrc.2012.01.027.

42. McHugh, D., Wager-Miller, J., Page, J., and Bradshaw, H.B. (2012). siRNA knockdown of GPR18 receptors in BV-2 microglia attenuates N-arachidonoyl glycine-induced cell migration. J. Mol. Signal. *7*, 10. https://doi.org/10.1186/1750-2187-7-10.

43. McHugh, D., Page, J., Dunn, E., and Bradshaw, H.B. (2012). Delta(9)-Tetrahydrocannabinol and N-arachidonyl glycine are full agonists at GPR18 receptors and induce migration in human endometrial HEC-1B cells. Br. J. Pharmacol. *165*, 2414–2424. https://doi.org/10.1111/j.1476-5381.2011.01497.x.

44. Grabiec, U., Hohmann, T., Ghadban, C., Rothgänger, C., Wong, D., Antonietti, A., Groth, T., Mackie, K., and Dehghani, F. (2019). Protective effect of N-arachidonoyl glycine-GPR18 signaling after excitotoxical lesion in murine organotypic hippocampal slice cultures. Int. J. Mol. Sci. *20*, 1266. https://doi.org/10.3390/ijms20061266.

45. Burstein, S.H., McQuain, C.A., Ross, A.H., Salmonsen, R.A., and Zurier, R.E. (2011). Resolution of inflammation by N-arachidonoylglycine. J. Cell. Biochem. *112*, 3227–3233. https://doi.org/10.1002/jcb.23245.

46. Console-Bram, L., Brailoiu, E., Brailoiu, G.C., Sharir, H., and Abood, M.E. (2014). Activation of GPR18 by cannabinoid compounds: a tale of biased agonism. Br. J. Pharmacol. *171*, 3908–3917. https://doi.org/10.1111/bph.12746.

47. Sotudeh, N., Morales, P., Hurst, D.P., Lynch, D.L., and Reggio, P.H. (2019). Towards A molecular understanding of the cannabinoid related orphan receptor GPR18: a focus on its constitutive activity. Int. J. Mol. Sci. *20*, 2300. https://doi.org/10.3390/ijms20092300.

48. Chi, H. (2012). Regulation and function of mTOR signalling in T cell fate decisions. Nat. Rev. Immunol. *12*, 325–338. https://doi.org/10.1038/nri3198.

49. Lieberman, L.A., Banica, M., Reiner, S.L., and Hunter, C.A. (2004). STAT1 plays a critical role in the regulation of antimicrobial effector mechanisms, but not in the development of Th1-type responses during toxoplasmosis. J. Immunol. *172*, 457–463. https://doi.org/10.4049/jimmunol.172.1.457.

50. Johnson, L.M., and Scott, P. (2007). STAT1 expression in dendritic cells, but not T cells, is required for immunity to Leishmania major. J. Immunol. *178*, 7259–7266. https://doi.org/10.4049/jimmunol.178.11.7259.

51. Tanaka, S., Yoshimoto, T., Naka, T., Nakae, S., Iwakura, Y.I., Cua, D., and Kubo, M. (2009). Natural occurring IL-17 producing T cells regulate the initial phase of neutrophil mediated airway responses. J. Immunol. *183*, 7523–7530. https://doi.org/10.4049/jimmunol.0803828.

52. Wishart, D.S., Feunang, Y.D., Marcu, A., Guo, A.C., Liang, K., Vázquez-Fresno, R., Sajed, T., Johnson, D., Li, C., Karu, N., et al. (2018). Hmdb 4.0: the human metabolome database for 2018. Nucleic Acids Res. *46*, D608–D617. https://doi.org/10.1093/nar/gkx1089.

53. Pang, Z., Chong, J., Zhou, G., de Lima Morais, D.A., Chang, L., Barrette, M., Gauthier, C., Jacques, P.É., Li, S., and Xia, J. (2021). MetaboAnalyst 5.0: narrowing the gap between raw spectra and functional insights. Nucleic Acids Res. *49*, W388–W396. https://doi.org/10.1093/nar/gkab382.

54. Le Belle, J.E., Harris, N.G., Williams, S.R., and Bhakoo, K.K. (2002). A comparison of cell and tissue extraction techniques using high-resolution 1H-NMR spectroscopy. NMR Biomed. *15*, 37–44. https://doi.org/10.1002/nbm.740.

55. McNally, B.D., Ashley, D.F., Hänschke, L., Daou, H.N., Watt, N.T., Murfitt, S.A., MacCannell, A.D.V., Whitehead, A., Bowen, T.S., Sanders, F.W.B., et al. (2022). Long-chain ceramides are cell non-autonomous signals linking lipotoxicity to endoplasmic reticulum stress in skeletal muscle. Nat. Commun. *13*, 1748. https://doi.org/10.1038/s41467-022-29363-9.

56. Smith, C.A., Want, E.J., O'Maille, G., Abagyan, R., and Siuzdak, G. (2006). XCMS: processing mass spectrometry data for metabolite profiling using nonlinear peak alignment, matching, and identification. Anal. Chem. *78*, 779–787. https://doi.org/10.1021/ac051437y.

57. Liggi, S., Hinz, C., Hall, Z., Santoru, M.L., Poddighe, S., Fjeldsted, J., Atzori, L., and Griffin, J.L. (2018). KniMet: a pipeline for the processing of chromatography-mass spectrometry metabolomics data. Metabolomics *14*, 52. https://doi.org/10.1007/s11306-018-1349-5.

58. West, J.A., Beqqali, A., Ament, Z., Elliott, P., Pinto, Y.M., Arbustini, E., and Griffin, J.L. (2016). A targeted metabolomics assay for cardiac metabolism and demonstration using a mouse model of dilated cardiomyopathy. Metabolomics *12*, 59. https://doi.org/10.1007/s11306-016-0956-2.

59. Adebayo, A.S., Roman, M., Zakkar, M., Yusoff, S., Gulston, M., Joel-David, L., Anthony, B., Lai, F.Y., Murgia, A., Eagle-Hemming, B., et al. (2022). Gene and metabolite expression dependence on body mass index in human myocardium. Sci. Rep. *12*, 1425. https://doi.org/10.1038/s41598-022-05562-8.

60. Han, B., Wright, R., Kirchhoff, A.M., Chester, J.A., Cooper, B.R., Davisson, V.J., and Barker, E. (2013). Quantitative LC-MS/MS analysis of arachidonoyl amino acids in mouse brain with treatment of FAAH inhibitor. Anal.Biochem. *432*, 74–81. https://doi.org/10.1016/j.ab.2012.09.031.

61. Levison, B.S., Zhang, R., Wang, Z., Fu, X., DiDonato, J.A., and Hazen, S.L. (2013). Quantification of fatty acid oxidation

products using online high-performance liquid chromatography tandem mass spectrometry. Free Radic. Biol. Med. *59*, 2–13. https://doi.org/10.1016/j.freeradbiomed.2013.03.001.

62. Pertea, M., Kim, D., Pertea, G.M., Leek, J.T., and Salzberg, S.L. (2016). Transcript-level expression analysis of RNA-seq experiments with HISAT, StringTie and Ballgown. Nat. Protoc. *11*, 1650–1667. https://doi.org/10.1038/nprot.2016.095.

63. Pertea, M., Pertea, G.M., Antonescu, C.M., Chang, T.-C., Mendell, J.T., and Salzberg, S.L. (2015). StringTie enables improved reconstruction of a transcriptome from RNA-seq reads. Nat. Biotechnol. *33*, 290–295. https://doi.org/10.1038/nbt.3122.

64. Frazee, A.C., Pertea, G., Jaffe, A.E., Langmead, B., Salzberg, S.L., and Leek, J.T. (2015). Ballgown bridges the gap between transcriptome assembly and expression analysis. Nat. Biotechnol. *33*, 243–246. https://doi.org/10.1038/nbt.3172.

65. Yu, G., Wang, L.-G., Han, Y., and He, Q.-Y. (2012). clusterProfiler: an R Package for comparing biological themes among gene clusters. OMICS A J. Integr. Biol. *16*, 284–287. https://doi.org/10.1089/omi.2011.0118.

66. Wu, T., Hu, E., Xu, S., Chen, M., Guo, P., Dai, Z., Feng, T., Zhou, L., Tang, W., Zhan, L., et al. (2021). clusterProfiler 4.0: a universal enrichment tool for interpreting omics data. Innovation *2*, 100141. https://doi.org/10.1016/j.xinn.2021.100141.

STAR★METHODS

KEY RESOURCES TABLE

REAGENT or RESOURCE	SOURCE	IDENTIFIER
Antibodies		
Purified anti-human CD3 Antibody	BioLegend	Cat#317301, RRID: AB_571926
Purified anti-human CD28 Antibody	BioLegend	Cat#302901, RRID: AB_314303
p70 S6 kinase antibody	Cell Signaling Technology	Cat#9202, RRID:AB_331676
Phospho-p70 S6 Kinase (Thr389) Antibody	Cell Signaling Technology	Cat#9205, RRID:AB_330944
S6 Ribosomal Protein (54D2) Mouse mAb	Cell Signaling Technology	Cat#2317, RRID:AB_2238583
Phospho-S6 Ribosomal Protein (Ser240/244) Antibody	Cell Signaling Technology	Cat#2215, RRID:AB_331682
Stat1 (9H2) Mouse mAb	Cell Signaling Technology	Cat#9176, RRID:AB_2240087
Phospho-Stat1 (Tyr701) (58D6) Rabbit mAb	Cell Signaling Technology	Cat#9167, RRID:AB_561284
Stat3 (124H6) Mouse mAb	Cell Signaling Technology	Cat#9139, RRID:AB_331757
Phospho-Stat3 (Tyr705) Antibody	Cell Signaling Technology	Cat#9131, RRID:AB_331586
β-Actin (8H10D10) Mouse mAb	Cell Signaling Technology	Cat#3700, RRID:AB_2242334
IRDye800CW Goat anti-rabbit IgG	Li-Cor Bioscience	Cat. #926-32211, RRID:AB_621843
IRDye680RD Donkey anti-mouse IgG	Li-Cor Bioscience	Cat. #926-68072, RRID: AB_10954628
IRDye680RD Goat anti-rabbit IgG	Li-Cor Bioscience	Cat. #926-68071, RRID: AB_10956166
Bacterial and virus strains		
GPR18 Human shRNA Lentiviral Particle (Locus ID 2841)	OriGene Technologies	Cat#TL312655V
Lenti-shRNA Control Particles	OriGene Technologies	Cat#TR30021V
Biological samples		
Human serum	From subject cohort - ClinicalTrials.gov ID-NCT02719899	N/A
Chemicals, peptides, and recombinant proteins		
Arachidonoyl Glycine	Cayman Chemical Company	Cat#90051; CAS: 179113-91-8
PSB-KD107	Cayman Chemical Company	Cat#31393; CAS: 955121-65-0
PSB-CB5	Tocris	Cat#6372; CAS: 1627710-30-8
Human IL-2 Recombinant protein	Peprotech	Cat#200-02B
Critical commercial assays		
Human $CD4^+$T cell Isolation Kit	Miltenyi Biotec	Cat#130-091-155
CyQUANT™ LDH Cytotoxicity Assay	Invitrogen	Cat#C20300
CyQUANT™ Cell Proliferation Assay	Invitrogen	Cat#C7026
Human IFNg Duoset ELISA Kit	R&D Systems	Cat#DY285B
Human IL-4 Duoset ELISA Kit	R&D Systems	Cat#DY204
Human IL-17 Duoset ELISA Kit	R&D Systems	Cat#DY317
Deposited data		
Human Metabolome Database (HMDB, Version 4.0)	Wishart et al.[52]	https://hmdb.ca/
RNAseq of PBMCs	This paper; Han et al.[13]	Table S3; GEO: GSE165149
RNAseq of subcutaneous adipose tissue biopsies	Rey et al.[35]	GEO: GSE166047

(*Continued on next page*)

Continued

REAGENT or RESOURCE	SOURCE	IDENTIFIER
Serum metabolomics data	This paper; Mendeley Data: https://data.mendeley.com/datasets/zvzvd5f5cb/1	Table S2; https://doi.org/10.17632/zvzvd5f5cb.1
Experimental models: Organisms/strains		
Human HealthyVolunteer	NIH Clinical Center Blood Bank (NCT00001846) and ClinicalTrials.gov ID-NCT01143454	N/A
Oligonucleotides		
GATA3	QIAGEN	Cat#QT00095501
RORC	QIAGEN	Cat#QT00097888
TBX21	QIAGEN	Cat#QT00042217
GPR18	QIAGEN	Cat#QT01001504
18S	QIAGEN	Cat#QT00199367
Software and algorithms		
Thermo Xcalibur (version 2.2)	Thermo Scientific	Cat#OPTON-30965
Image Studio (version 5.2)	LI-COR	https://www.licor.com/bio/image-studio/
MetaboAnalyst (version 5.0)	Pang, et al.[53]	https://www.metaboanalyst.ca/
Prism (version 9)	GraphPad Software	https://www.graphpad.com/
Simca (version 17)	Umetrics	https://www.sartorius.com/en/products/process-analytical-technology/data-analytics-software/mvda-software/simca
Ingenuity Pathway Analysis	QIAGEN	https://digitalinsights.qiagen.com/products-overview/discovery-insights-portfolio/analysis-and-visualization/qiagen-ipa/
R and R Studio	Free Software	http://www.r-project.org/
Other		
Code used to process and analyze RNAseq data	Han et al.[13]	https://github.com/NHLBI-BCB/PTNA

RESOURCE AVAILABILITY

Lead contact

Further information and requests for resources and reagents should be directed to and will be fulfilled by the lead contact, Michael N. Sack (sackm@nih.gov).

Materials availability

This study did not generate new unique reagents.

Data and code availability

- This paper analyzes existing, publicly available RNA sequencing data. Metabolomic and lipidomic data generated by this study was deposited in the Mendeley Data repository and the accession number for the datasets are listed in the key resources table.
- This paper does not report original code.
- Any additional information required to reanalyze the data reported in this paper is available from the lead contact upon request.

EXPERIMENTAL MODEL AND SUBJECT DETAILS

Fasting/re-feeding study

A clinical study (NCT02719899) was conducted to assess the immunologic effects of a 24-hour fast and a re-feeding period on normal volunteers, as previously described.[13] The National Heart, Lung, and Blood Institute (NHLBI) Institutional Review Board approved this study, and volunteers signed informed consent before participation. 10 males and 11 females, aged 2229, with no acute or chronic disease and a normal-weight BMI were included in this study. Study participants then consumed a fixed 500-calorie morning meal before 8 a.m. and began a 24-hour total fast before drawing fasting blood. Study participants then consumed another 500-calorie morning meal, and after 3 hours, the re-feeding serum and peripheral blood mononuclear cells (PBMCs) samples were collected (t = 27 hours). A schematic of the clinical protocol is shown in Figure S1A. The demographics of the study subjects and the biochemical markers, including glucose, insulin, and growth hormone levels that support the distinct nutrient loads in the fasted *versus* the refed state are shown in Table S1.

Lean/obese study

PBMCs from lean and obese volunteers were collected under the Disease Discovery Natural History Protocol (NCT01143454). The National Heart, Lung, and Blood Institute (NHLBI) Institutional Review Board approved this study, and volunteers signed informed consent before participation. 30 African American female volunteers aged 24-78 were recruited for this study. 15 volunteers with an average BMI of 24.17 $\pm$ 2.17 and an average age of 53.73 $\pm$ 18.49 were classified as lean. 15 volunteers with an average BMI of 40.29 $\pm$ 8.06 and an average age of 53.00 $\pm$ 12.45 were classified as obese.

Healthy volunteers

The blood from healthy volunteers for functional validation of target proteins was obtained from either a Disease Discovery Natural History (NCT01143454) or NIH Clinical Center blood bank (NCT00001846) protocol.

METHOD DETAILS

LC-MS of serum samples

Sample processing

The samples were extracted using a standard methanol-chloroform-water extraction on ice.[54] The aqueous fraction and organic fraction were separated for use in the following experiments. All solvents were analytical grade or HPLC-MS quality for the following methods and sourced from Sigma-Aldrich.

Open profile lipidomics of serum

Serum lipidomics methods were adapted from the methods described by McNally et al.[55] The extracted organic fraction was reconstituted in 250 µL internal standard solution containing the following deuterated standards at 2.5 µg/mL in 1:1 chloroform-methanol: C16-D_{31} Ceramide, 16:0-D_{31}-18:1 PA, 16:0-D_{31}-18:1 PC, 16:0-D_{31}-18:1 PE, 16:0-D_{31}-18:1 PG, 16:0-D_{31}-18:1 PI, 14:0 PS-D_{54}, and 16:0-D_{31} SM (Avanti Polar Lipids); and 18:0-D_6 CE, 15:0-D_{29} FA, 17:0-D_{33} FA, 20:0-D_{39} FA, 14:0-D_{29} LPC-D_{13}, 45:0-D_{87} TG, 48:0-D_{83} TG, and 54:0-D_{105} TG (CDN Isotopes/QMX Laboratories). Samples with internal standards were dried under nitrogen and re-solubilized in 100 µL 1:1 methanol-chloroform solution; 10 µL was then transferred to a 1.5 mL glass vial containing 190 µl of 2:1:1 isopropanol-acetonitrile-water solution. 10 mM ammonium formate was added to solvents in positive ionization mode, and 10 mM ammonium acetate was added to solvents in negative ionization mode. Mass spectrometry was performed using an Orbitrap Velos Elite Mass Spectrometer (Thermo Scientific) in positive and negative ionization mode with electrospray ionization. 5 µL of each sample was injected onto a 75 µM x 100 mm C18 packed-tip column (Thermo Scientific) conditioned at 55°C. The mobile phase consisted of: (A) a 60:40 acetonitrile-water solution and (B) a 10:90 acetonitrile-isopropanol solution. Spectra were converted from Xcalibur .raw files into .mzML files for peak identification and analysis within XCMS software using R studio.[56] Annotation was performed with an R script using accurate mass,[57] and peak intensity was normalized to the corresponding internal standard for the lipid species. Analytes that could not be annotated were excluded from further analysis. Missing values were treated as the result of low signal intensity and thus imputed using 20% of the minimum value of the variable. Lipid species containing more than one-third of missing variables were excluded from the dataset.

Targeted detection of polar metabolites in serum

Serum metabolomics methods were adapted from the methods described by West et al.[58] and Adebayo et al.[59] For reverse-phase analysis, the extracted aqueous fraction was reconstituted in 100 μL of a 10 mM solution of ammonium acetate in water containing a mixture of internal standards at a concentration of 10 μM: proline, valine-D8, leucine-D10, lysine-U-13C, glutamic acid-13C, phenylalanine-D5, succinic acid-D3, and serotonin-D4. Chromatography was performed with an ACE Excel 2 C18 PFP (100A. 150 x 2.1 mm 5μm) column conditioned at 30°C. The mobile phase consisted of: (A) a 0.1% solution of formic acid in water and (B) a 0.1% formic acid solution in acetonitrile. For normal phase analysis, the aqueous fraction was reconstituted in 100 μL of a 7:3 solution of acetonitrile and 10 mM ammonium carbonate in water containing a mixture of internal standards at a concentration of 10 μM: glutamic acid-13C, succinic acid-D3, and AMP. Chromatography was performed with a BEHAmide (150 x 2.1 mm 1.7 μm) column conditioned at 30°C. The mobile phase consisted of: (A) a 0.1% solution of ammonium carbonate in water and (B) acetonitrile. Targeted MS/MS was performed with a Thermo Scientific Vanquish UHPLC+ coupled to a TSQ Quantiva mass spectrometer (Thermo Fisher Scientific). The electrospray ionization (ESI) source was operated in positive and negative ionization mode, with the electrospray voltage set to 3500 V for the positive ionization and 2500 V for the negative ionization. Nitrogen at 48 mTorr and 420°C was used as a drying gas for solvent evaporation. Data acquisition and processing were performed using Thermo Xcalibur software (version 2.2; Thermo Scientific). Peak intensity was normalized to appropriate internal standards.

Targeted detection of N-arachidonylglycine in serum

A targeted method of detecting NAGly by LC-MS/MS was performed as described by Han et al.[60] Serum samples from n = 5 volunteers were prepared with 1000 ppm of a D8-arachidonic acid internal standard in acetonitrile. Samples were homogenized and centrifuged, and the supernatant was collected with 0.1% trifluoroacetic acid in water. Solid-phase extraction with a Bond Elut-C8, 200 mg, 3MI SPE column (Agilent) was used to improve detection sensitivity. Targeted analyses were performed with a Thermo Scientific UHPLC+ coupled to a TSQ Quantiva Triple Quadrupole mass spectrometer. The sample was injected into a CSH C18 (1.7 μM x 100 mm) HPLC column (Acquity) maintained at 45°C with an injection volume of 10 μl. The mobile phase consisted of (A) 0.1% formic acid in water and (B) 0.1% formic acid in acetonitrile. The ESI source was operated in negative mode with an electrospray voltage of 2500 V. Data acquisition and processing were performed as described for polar metabolites. Individual peaks were integrated and normalized to the arachidonic acid internal standard.

Targeted detection of N-arachidonylglycine in cell culture media

Cell culture media was extracted with 10% acetic acid in 2:20:30 water/isopropanol/hexane as described by Levison et al.[61] The hexane layer was evaporated to dryness and reconstituted in 85% methanol in water. Targeted detection was performed by the NHLBI Biochemistry Core using an Agilent 1100 HPLC coupled to an Agilent G1956B single-quadrupole mass spectrometer. The sample was injected into a Zorbax XDB-Phenyl, 2 μM x 50 mm column (Agilent) with an injection volume of 5 μM. The mobile phase consisted of (A) 0.1% formic acid in dH_2O and (B) 0.1% formic acid in acetonitrile.

Computational analysis of metabolomics data

Univariate analysis of serum metabolomics and lipidomics data were performed in MetaboAnalyst (version 5.0, https://www.metaboanalyst.ca/)[53] and Prism (version 9, GraphPad Software). Supervised multivariate analysis was performed with orthogonal partial least squares-discriminant analysis (OPLS-DA) using Simca® software (version 17; Umetrics), and model performance is reported using R^2X, R^2Y, and Q^2. The model was validated using cross-validation analysis of variance (CV-ANOVA) and permutation. Variables important for prediction (VIP) were reported for the OPLS-DA model, and a heatmap of relative expression in the fasted and refed sample groups was generated using Prism (version 9, GraphPad Software). Metabolites were annotated using the Human Metabolome Database (HMDB, Version 4.0, https://hmdb.ca/).[52] Canonical pathway and network enrichment analysis of metabolites significantly different between fasting and re-feeding ($p < 0.05$) was performed using the metabolomics analysis module in Ingenuity Pathway Analysis (IPA, QIAGEN). Networks were generated using the Pathway Designer tool in IPA.

Computational analysis of transcriptomics data

RNA sequencing (RNAseq) of PBMCs isolated from human volunteers that underwent the 24-hour fasting and re-feeding study was performed as previously described by Han et al. (GSE165149).[13] RNAseq analysis of subcutaneous adipose tissue biopsies collected from human volunteers classified as lean or obese has been previously described by Rey et al. (GSE166047).[35] Data were accessed from the GEO repository. RNA-seq data from both studies were processed and re-analyzed by the NHLBI Bioinformatics Core as previously described,[13] using a missing value cutoff of 50% for samples with FPKM greater than 1. Gene expression levels were quantified using StringTie (https://github.com/gpertea/stringtie).[62,63] Genes differentially expressed between fasting and re-feeding samples or lean and obese samples were evaluated using Ballgown (http://bioconductor.org/packages/release/bioc/html/ballgown.html).[64] Functional enrichment analysis of differentially expressed genes was performed using clusterProfiler (https://bioconductor.org/packages/release/bioc/html/clusterProfiler.html).[65,66] Differentially expressed genes were mapped to biological process and molecular function enrichment using annotations provided by the GO database (http://geneontology.org/).[22,23] Genes annotated for the G-protein coupled receptor signaling pathway (GO: 0007186) were extracted from the 24-hour fasting and re-feeding RNAseq dataset, and a heatmap of log-transformed gene expression was generated in R (https://www.R-project.org/).

Functional validation in primary CD4$^+$T cells

Primary CD4$^+$T cells from whole blood

Functional validation was performed using blood from healthy volunteers donated to the National Institutes of Health Clinical Center blood bank (ClinicalTrials.gov ID: NCT00001846) as described previously.[13] In brief, primary PBMCs were isolated from whole blood and CD4$^+$T cells were isolated by negative using a human CD4$^+$T Cell Isolation Kit (Miltenyi Biotec). Primary CD4$^+$T cells were cultured in Roswell Park Memorial Institute (RPMI) 1640 medium (Invitrogen) supplemented with 25 mM of HEPES buffer, 10% heat-inactivated FBS, and penicillin-streptomycin at a density of 2x10^6 cells/mL. T cell receptor (TCR) activation was performed with a 3-day incubation on sterile cell culture plates that had been pre-coated with 5 μg/ml αCD3 and 10 μg/ml αCD28 antibodies (BioLegend) overnight at 4°C.

NAGly and receptor ligand cell studies

Cells were treated with either 10 μM NAGly (Cayman Chemical) or ethanol control for 3 days. The GPR18 agonist PSB-KD107 (Cayman Chemical Company) and the GPR18 antagonist PSB-CB5 (Fischer Scientific) were prepared as stock solutions in DMSO. Cells were treated with 10 μM PSB-KD107, 10 μM PSB-CB5, or DMSO control for 3 days. On the third day, cells were centrifuged, and the supernatant was collected for enzyme-linked immunosorbent assay (ELISA) assay. Cells were washed with PBS and used for subsequent Western blot or RNA extraction. Cytotoxicity was assessed using the CyQUANT™ LDH Cytotoxicity Assay (Invitrogen).

Genetic knockdown experiments

Lentiviral knockdown was performed using gene-specific human shRNA lentiviral particles (GPR18: Locus ID 2841) or negative control scrambled shRNA lentiviral particles (Origene Technologies). A set of four distinct 29-mer shRNA was provided, and the optimal selection for GPR18 mRNA knockdown efficiency was assessed by qRT-PCR. Before lentiviral introduction, 2.5x10^6/mL of CD4$^+$T cells were pre-conditioned with cell culture media containing 8 ng/mL of DEAE-Dextran (Sigma-Aldrich), 8 ng/mL of polybrene (Sigma-Aldrich), and 50 ng/mL of IL-2 (PeproTech) for 30 min. For every 5x10^6 cells, 25 μL of >10^7 TU/mL lentivirus were introduced into the media. After a 24-hour incubation, cells were plated with fresh cell culture media at 1x10^6 cells/mL on αCD3/αCD28 antibody-coated plates for 3 days. For GPR18 knockdown, cells were treated with either 10 μM NAGly or ethanol control for the 3-day activation period.

ELISA immunoassay

After activation and treatment, cell supernatants were collected for cytokine assay, and cell pellets were reserved for normalization. The cytokines IFNγ, IL-4, and IL-17, were measured by ELISA kits (R&D Systems), and results were collected using a microplate reader. Cytokine levels were normalized to cell density using the CyQUANT™ Cell Proliferation Assay (Invitrogen) or the bicinchoninic acid (BCA) protein assay (Pierce).

Immunoblot analysis

Protein was extracted from $CD4^+$T cells in radioimmunoprecipitation assay (RIPA) buffer and supplemented with protease and phosphatase inhibitors (Pierce) and kept on ice to maintain protein integrity. Protein concentration was measured using the BCA protein assay (Pierce). Protein lysates were denatured using Laemmli SDS sample buffer and boiled at 95°C for 5 min before separation on a NuPAGE™ 4-12% Bis-Tris gel (Invitrogen) in NuPAGE™ MES SDS running buffer (Invitrogen). The gel was transferred to a nitrocellulose membrane (Bio-Rad Laboratories) using a Trans-Blot Turbo Transfer System (Bio-Rad Laboratories). Membranes were blocked with Intercept® Tris-buffered saline (TBS) Blocking Buffer (LI-COR) for 1 hour at room temperature. Overnight, membranes were then incubated in mouse or rabbit primary antibody (1:1,000 dilution) on a 4°C shaker. The next day, membranes were washed using PBS-Tris and incubated in anti-mouse or anti-rabbit secondary antibody (1:10,000 dilution) conjugated with IRDye 800CW or IRDye 680RD (LI-COR) for 1 hour at room temperature. Membrane scanning and image capture were performed using an Odyssey CLx Imaging System (LI-COR), and protein band intensity was quantified using Image Studio software (version 5.2, LI-COR). Primary antibodies for each steady-state protein and associated phosphoprotein included P70S6 kinase and pP70S6 kinase (T389), S6 and pS6 (S240/244), STAT1 and pSTAT1 (Y701), and STAT3 and pSTAT3 (Y705) (Cell Signaling Technology). β-actin (Cell Signaling Technology) was used as a loading control. Western blots were quantified by normalizing band intensity to the β-actin loading control, and phosphoprotein abundance was quantified relative to the associated steady-state protein.

Quantitative RT-PCR

RNA was isolated from $CD4^+$T cells using the NucleoSpin RNA kit (Macherey-Nagel). Complementary DNA (cDNA) was synthesized using the SuperScript III First-Strand Synthesis kit (Invitrogen). Quantitative real-time PCR (qRT-PCR) was prepared using the SYBR Green FastStart Essential DNA Master Mix (Roche) and performed on a LightCycler 96 (version 1.1; Roche). The following human gene specific QuantiTect primer assays (QIAGEN) were used: GATA3 (QT00095501), RORC (QT00097888), TBX21 (QT00042217), GPR18 (QT01001504), and 18S (QT00199367). Target gene Ct values were normalized to 18S expression using the $2^{-\Delta\Delta Ct}$method.

QUANTIFICATION AND STATISTICAL ANALYSIS

Pairwise hypothesis testing of metabolomics and transcriptomics data was performed using a Wilcoxon signed-rank test. There were 21 paired samples in the fasting and re-feeding groups. Multiple testing corrections were performed for metabolomics and transcriptomics analysis, and q-values are reported in Tables S2 and S3. Biological study statistics were performed in Prism (version 9, GraphPad Software). The number of biological replicates is reported as *n* in each figure legend, and each biological replicate was performed on cells isolated from a distinct whole blood sample. Each biological replicate represents the mean of technical replicates performed in duplicate. Dot plots contain every biological replicate, and error bars show the standard error of the mean. Parametric hypothesis testing was performed using a Student's *t*-test when comparing two group means and an ANOVA with multiple comparisons test when comparing three or more group means. Statistical tests and resulting p-values are reported in each figure legend. Statistical significance was interpreted as a p-value < 0.05.

ADDITIONAL RESOURCES

Clinical study NCT02719899: https://clinicaltrials.gov/ct2/show/NCT02719899.